

# Multi-material distributed recycling via Fused granular fabrication: rHDPE and rPET case of study

Catalina Suescun Gonzalez<sup>12</sup>, Fabio A. Cruz Sanchez<sup>1</sup>, Hakim Boudaoud<sup>1</sup>, Cécile Nouvel<sup>2</sup>, Joshua Pearce<sup>3</sup>

<sup>1</sup>Université de Lorraine – ERPI – F-54000, Nancy, France

<sup>2</sup>Université de Lorraine, CNRS, LRGP, F-54000 Nancy, France

<sup>3</sup>Western University, Department of Electrical & Computer Engineering, Canada, London

## Abstract

The high volume of plastic waste and the extremely low recycling rate has created a serious challenge worldwide. Local distributed recycling coupled to additive manufacturing (DRAM) offers a solution by economically incentivizing local recycling. A new DRAM technology capable of processing large quantities of plastic waste quickly is fused granular fabrication (FGF), where solid shredded plastic waste can be reused directly as 3D printing feedstock. This study presents an experimental assessment of multi-material recycling printability, using two of the most common thermoplastics in the beverage industry polyethylene terephthalate (PET) and high-density polyethylene (HDPE) and the feasibility of mixing PET and HDPE to be used as a feedstock material for large-scale 3-D printing. After the material collection, shredding, and cleaning its characterization, and optimization of parameters for 3D printing was performed. Results showed the feasibility of printing a large object from rPET/rHDPE flakes reducing the production cost up to 88%.

# Acronyms

Acronym	Definition
<b>ABS</b>	Acrylonitrile Butadiene Styrene
<b>AM</b>	Additive Manufacturing
<b>DRAM</b>	Distributed recycling via additive manufacturing
<b>DSC</b>	Differential scanning calorimetry
<b>FDM</b>	Fused deposition modeling
<b>FFF</b>	Fused filament fabrication
<b>FGF</b>	Fused granular fabrication
<b>FPF</b>	Fused particle fabrication
<b>FTIR</b>	Fourier-transform infrared spectroscopy
<b>HDPE</b>	High-density polyethylene
<b>MFI</b>	Melt flow index
<b>PC</b>	Polycarbonate
<b>PET</b>	Poly(ethylene terephthalate)
<b>PLA</b>	Poly(lactic acid)
<b>PP</b>	Polypropylene
<b>PSO</b>	Particle swarm optimization
<b>PS</b>	Polystyrene
<b>SEBS</b>	Poly (styrene-block-ethene-co-butene-block-styrene)
<b>Tg</b>	Glass temperature
<b>pBC</b>	Printed Bottle-Cap
<b>rHDPE</b>	Recycled High-density Polyethylene
<b>rPET90//rHDPE10</b>	Recycled Bottle-Cap (Cristaline bottle shredded without separation)
<b>rPET</b>	Recycled Poly(ethylene) terephthalate
<b>vPET</b>	Virgin or commercial Poly(ethylene terephthalate)

## 1 Introduction

- <sup>1</sup> The disposal of plastic waste is one of the most challenging current environmental concerns  
<sup>2</sup> given its systemic complexity ([Evode et al., 2021](#)). The mass of micro- / meso- plastics in the  
<sup>3</sup> oceans are expected to exceed the mass of the global stock of fish by 2050 ([MacArthur, 2017](#)).  
<sup>4</sup> More critically, the global plastic annual production is expected to reach 1100 metric tons  
<sup>5</sup> by the same year ([Geyer, 2020](#)). The societal awareness on plastic recycling have received  
<sup>6</sup> substantial attention by scientific, policymaker and general public ([Soares et al., 2021](#)). Un-  
<sup>7</sup> fortunately, the statistical analysis on the centralized recycling process proves that it has  
<sup>8</sup> been largely ineffective ([Siltaloppi and Jähi, 2021](#)) as only 9% of the plastic that has been  
<sup>9</sup> produced has been recycled from the total stock produced since 1950 ([Geyer et al., 2017](#)).  
<sup>10</sup> Therefore, it remains an open challenge to identify alternatives to valorize discarded plastic

11 material.

12 Distributed recycling and additive manufacturing (DRAM), is an innovative technical ap-  
13 proach to recycle plastic wastes (Cruz Sanchez et al., 2020; Dertinger et al., 2020). DRAM  
14 was first practiced with recyclebots, which are waste plastic extruders that made filament  
15 for conventional fused filament-based 3-D printers (Baechler et al., 2013; Woern et al., 2018;  
16 Zhong and Pearce, 2018). Past research demonstrated that using distributed recycling fits  
17 into the circular economy paradigm (Despeisse et al., 2017; Ford and Despeisse, 2016); where  
18 consumers directly recycle their own waste into consumer products from open source designs,  
19 from toys for children (Petersen et al., 2017) to adaptive aids for those with arthritis (Gallup  
20 et al., 2018). Distributed manufacturing is now in wide use (Pearce and Qian, 2022). In  
21 this way DRAM-based recycling is done in a closed loop supply chain network (Santander et  
22 al., 2020). This type of recycling aims to reduce the environmental impact by the reduction  
23 of the transportation from the waste source to recycling facilities (Kreiger et al., 2014). In  
24 that sense, it aims to propose innovative closed-loop strategies using waste materials as raw  
25 resources (Romani et al., 2021).

26 Fused filament fabrication (FFF, which is also known as Fused Deposition Modelling –FDM©–  
27 ) is the most-widespread and established extrusion-based AM technology due to the open  
28 source proliferation from the self-replicating rapid prototyper (RepRap) project (Bowyer,  
29 2014; Jones et al., 2011; Sells et al., 2009). This is due to its simplicity, versatility, low-  
30 cost, and ability in the construction of geometrically complex objects in the industrial and  
31 prosumer domains (Romani et al., 2021). Indeed, the open-source 3-D approach for 3-D  
32 printers has enabled the technology to evolve in a radical manner for manufacturing and  
33 prototyping adding value to the recycled material (Cruz Sanchez et al., 2020). There are  
34 large efforts to find sustainable feedstocks for 3-D printing Pakkanen et al. (2017a). Several  
35 studies in the literature have increase the spectrum of recycled filament materials such as  
36 PLA (Anderson, 2017; Cruz Sanchez et al., 2017), ABS (Mohammed et al., 2017b, 2017a),  
37 PET (Vaucher et al., 2022; Zander et al., 2018), HDPE (Baechler et al., 2013; Chong et al.,  
38 2017; Mohammed et al., 2017b) PC (Gaikwad et al., 2018). In fact, using a comparative life

39 cycle assessment in a low density population case study of Michigan (USA), Kreiger et al.  
40 (2014) argued that about of 100 billion MJ of energy per year could be saved in a distributed  
41 approach, for the 984 million pounds of HDPE that are recycled in the U.S. There is thus  
42 considerable evidence that DRAM can reduce the energy consumption and greenhouse gases  
43 of the manufacturing processes.

44 Most DRAM studies have been using mono-material for the fabrication of feedstock for  
45 FFF. There are, however, several examples of mixed materials including wood waste and  
46 recycled plastic (Löschke et al., 2019; Pringle et al., 2018) and textile fibers and recycled  
47 plastic (Carrete et al., 2021). Recently, Zander et al. (2019) reported the manufacturing  
48 of composite filament from recycled PET/PP and PS/PP blending through compatibilizer  
49 copolymer such as SEBS. Their results revealed the technical printability of polypropylene  
50 blend composite filaments from a thermo-mechanical characterization perspective. Increasing  
51 the performance window of blending materials by compatibilization which could be a relevant  
52 path for recycling plastics in a local level and isolated areas contexts (e.g. during humanitarian  
53 crises (Savonen et al., 2018 ; Corsini et al., 2022 ; Lipsky et al., 2019), supply chain disruptions  
54 (Attaran, 2020; Choong et al., 2020 ; Novak and Loy, 2020; Salmi et al., 2020 ) and/or isolated  
55 off-grid situations using solar-powered 3-D printers (Gwamuri et al., 2016 ; King et al., 2014;  
56 Mohammed et al., 2018; Wong, 2015)). Likewise, Vaucher et al. (2022) studied the evaluation  
57 of the microstructure, mechanical performance, and printing quality of filaments made from  
58 rPET and rHDPE varying the wt% of HDPE material from 0 to 10%. They confirmed the  
59 increase in the Young's modulus from 1.7 GPa of the pure PET to 2.1 GPa for all the HDPE  
60 concentrations. Additionally, the maximum stress of the bends were augmented with high  
61 HDPE concentrations. Values were lower than virgin PET filament, yet similar to commercial  
62 recycle ones. The addition of rHDPE at higher levels, however, helped to meet the brittle-  
63 ductile transition in 15% despite the low interfacial tension of both polymers, allowing the  
64 printing of quality parts.

65 While former studies have proven been successful in FFF, a new approach to DRAM is  
66 fused granular fabrication (FGF) or fused particle fabrication (FPF), where the material-

67 extrusion AM systems print directly from pellets, granules, flakes, shred or grinder material  
68 (Fontana et al., 2022; Woern et al., 2018). In the context of recycling, this could reduce the  
69 number of melt/extrusion cycles that degrade the material needed in the filament fabrication  
70 process (Cruz Sanchez et al., 2017). The FGF technique opens up the potential of use recycle  
71 materials as well as print large-scale objects either with a conventional cartesian 3-D printer  
72 (Woern et al., 2018), delta 3-D printer (Grassi et al., 2019) or hangprinter (Petsiuk et al.,  
73 2022; Rattan et al., 2023). Research groups corroborate that plastic waste can be used  
74 as feedstock materials for FGF/FPF. Alexandre et al. (2020) assessed the technical and  
75 economical dimensions of virgin and shredded PLA printed in a self-modified FGF machine  
76 and compared with FFF. The investigation showed that the use of FGF reduced printing cost,  
77 time and its mechanical performance was comparable with the obtained using the traditional  
78 FFF technique. Likewise, Woern et al. (2018) found comparable properties between PLA,  
79 ABS, PP, and PET recycled and virgin materials. Later publications demonstrated the  
80 technical and economic feasibility through the printing of complex objects validating the  
81 possibility of recycle plastic with FGF in both conventional and common FFF materials  
82 (Byard et al., 2019), but also recycle PC (Reich et al., 2019) and rPET (Little et al., 2020,).  
83 Few researchers, however, have addressed the problem of the direct printing of recycled  
84 multi-materials, which might be a key step forward needed to facilitate the ease of sorting  
85 and recycling post-consumer plastic waste materials.

86 This study explores the potential of direct 3-D printing two immiscible polymers commonly  
87 used in the beverage sector through a distributed recycling process for its easily implementa-  
88 tion operation at the local level. To demonstrate the feasibility of the process, the bottle water  
89 plastic most used in France of roughly 90% of PET (body of the bottle) and 10% of HDPE  
90 (cap) now called *rPET90//rHDPE10*, is used as a test material. The experimental process of  
91 collection, characterization, and printing of the recycled material is described and the results  
92 are discussed in the context of widespread DRAM adoption at the community-based level.

## 93 2 Materials and Methods

94 The methodology presented in Figure 1 outlines the approach adopted to develop the study.  
95 The three stages *Material obtention*, *Printing process* and *Evaluation* were thoroughly studied  
96 in order to control the major processes steps and the technical characterization methods. In  
97 the following subsections, each step is explained.

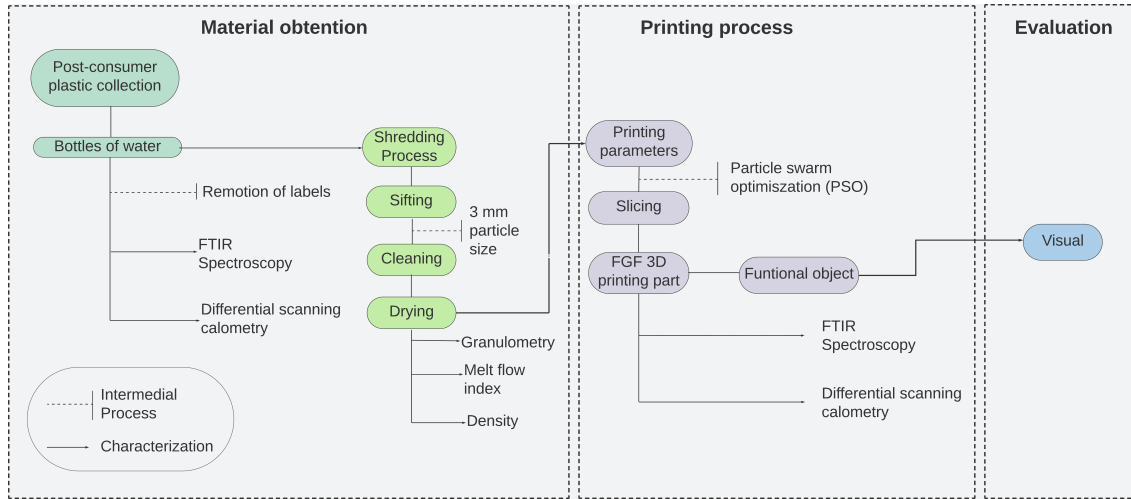


Figure 1: Global framework of the study

### 98 2.1 Raw material obtention

99 The goal of material stage is the collection and preparation of post-consumer plastic source. In  
100 this study, bottles of water coming from the French brand Cristaline<sup>®</sup> was used as a feedstock.  
101 The process steps used are shown in Figure 2 a/b. Post-consumer bottles were collected by  
102 receptacles placed in partnership schools in Lorraine, France. To convert the complete water  
103 bottles with its cap into 3DP feedstock material, the labels were removed before shredding  
104 in a cutting mill Retsch MS300 using a 3 mm grid. After shredding, the obtained flakes were  
105 sifted with a 1.5 mm, 3 mm, 5 mm sifters for further analysis. Next, flakes were cleaned  
106 with hot water in an ultrasonic machine at 60°C for 1h to remove contaminants. Lastly, they  
107 were dried in a conventional oven overnight at 80°C (Taghavi et al., 2018; Van de Voorde et  
108 al., 2022) to avoid degradation of the material. Washing conditions were the same for all the

109 samples, therefore, the effect of contaminants was not considered. The resultant material is  
110 shown in Fig 2.c.



Figure 2: Process steps to prepare the collected material

111 The material composition was calculated as a function of the mass of the bottles and caps  
112 separately. The percent (%) of bottle-cap was found to be ~90% rPET (bottle) and ~10%  
113 rHDPE (cap). The complete bottle was shredded without separation of both materials thus  
114 this percentage is constant for all the samples.

## 115 2.2 Material preparation and characterization

### 116 2.2.1 Material particle size analysis -Granulometry-

117 In order to ensure the particle size suitable for printing, the characterization of the granulate  
118 particles were developed using the open-source ImageJ software ([ImageJ, 2023](#)). The size  
119 characteristics of the particles were evaluated between four different samples; vPET (used as  
120 a reference) and the raw material sifted in three different sizes 1.5 mm, 3 mm and 5 mm.

<sup>121</sup> **2.2.2 Fourier-transform infrared spectroscopy –FTIR-**

<sup>122</sup> FTIR spectroscopy was carried out to determine the nature of the bottle and determine  
<sup>123</sup> if there were impurities, plasticizers or additives that could be detected. The analysis were  
<sup>124</sup> made on samples of rPET and rHDPE separately and then a printed sample of both materials  
<sup>125</sup> to determine if there was possible to observe a chemical bonding. Every sample was measured  
<sup>126</sup> in two different points, three times in each point then curves were normalized and analyzed  
<sup>127</sup> with the Origin Pro 8. The Fourier transform infrared spectra have been recorded in the range  
<sup>128</sup> of  $4000\text{ cm}^{-1}$  to  $375\text{ cm}^{-1}$  with resolution  $4\text{ cm}^{-1}$  using Bruker IFS 66V spectrophotometer.

<sup>129</sup> **2.2.3 Differential scanning calorimetry –DSC-**

<sup>130</sup> Differential scanning calorimetry analysis were performed with a DSC-1 Mettler Toledo with  
<sup>131</sup> STArE software operating under nitrogen atmosphere at heating rate and cooling rate of  
<sup>132</sup>  $10\text{ }^{\circ}\text{C/min}$ . rPET, rHDPE and rPET90//rHDPE10 samples were investigated using three  
<sup>133</sup> cycles: first heating from  $20^{\circ}\text{C}$  to  $270\text{ }^{\circ}\text{C}$ , cooling to  $20\text{ }^{\circ}\text{C}$  and reheating to  $270^{\circ}\text{C}$ . The  
<sup>134</sup> rHDPE sample was analyzed following similar cycles but with the maximum temperature set  
<sup>135</sup> at  $250^{\circ}\text{C}$  and the blend with temperatures from -20 to  $270^{\circ}\text{C}$ . Glass transition temperature  
<sup>136</sup> ( $T_g$ ) of rPET was determined during the first heating cycle, while rPET90//rHDPE10 ( $T_g$ )  
<sup>137</sup> during the second heating cycle along with the melting point of all materials. Crystallization  
<sup>138</sup> temperature ( $T_c$ ) of the each of the materials was determined during the cooling cycle. The  
<sup>139</sup> degree of crystallinity ( $X_c$ ) was calculated from the second cycle for recycled materials and  
<sup>140</sup> first cycle for the blend as expressed in equation (1) ([Pan et al., 2020](#); [Taghavi et al., 2018](#)):

$$X_c(\%) = \frac{\Delta H_m}{w \cdot \Delta H_m^{\circ}} \quad (1)$$

<sup>141</sup> Where,  $\Delta H_m$  is the latent heat of melt,  $w$  is weight percentage of polymer in the blend,  
<sup>142</sup> and  $\Delta H_m^{\circ}$  is the reference heat of 100% crystalline PET ( $140\text{ J/g}$ ) and HDPE ( $293\text{ J/g}$ ),  
<sup>143</sup> respectively, provided in the literature ([Kratofil et al., 2006](#); [Pan et al., 2020](#)).

<sub>144</sub> **2.2.4 Melt Flow Index –MFI-**

<sub>145</sub> The melt-flow index (MFI) of rPET90//rHDPE10 flakes was determined using a Instron  
<sub>146</sub> CEAST MF20. The analysis was performed using three samples of ~5 g at 255 °C using  
<sub>147</sub> a 2.16 kg weight according to ASTM D1238. The process was repeated three times. The  
<sub>148</sub> average value of the three results was then reported with *gr/10 × min* unit.

<sub>149</sub> **2.2.5 Density**

<sub>150</sub> In order to calculate the material's density, first; the volume was found measuring the dimen-  
<sub>151</sub> sions of a solid 50x50x50 mm cubic geometry fabricated injecting rPET90//rHDPE10 flakes  
<sub>152</sub> into a square mould with a known volume using open-source desktop injection (Holipress,  
<sub>153</sub> Holimaker, France) machine. Then the model was weighed, and the mass was obtained. Fi-  
<sub>154</sub> nally, density was calculated as expressed in Equation 2. To ensure the accuracy the test  
<sub>155</sub> was performed twice and the average value was reported in *g/cm<sup>3</sup>*.

$$\rho = V/m \quad \left[ \frac{g}{cm^3} \right] \quad (2)$$

<sub>156</sub> Where,  $\rho$  is the density,  $V$  is the volume, and  $m$  the mass.

<sub>157</sub> Afterwards, experimental results were compared with the theoretical blend density which  
<sub>158</sub> could be calculated by Equation 3.

$$\rho_{12} = \frac{1}{\frac{W_1}{\rho_1} + \frac{W_2}{\rho_2}} \quad \left[ \frac{g}{cm^3} \right] \quad (3)$$

<sub>159</sub> Where,  $\rho_{12}$  is the density of the blend,  $W_1$  and  $W_2$ , the weight fractions of each polymer,  $\rho_1$   
<sub>160</sub> and  $\rho_2$ , the theoretical density of each polymer for PET ( 1.38 *g/cm<sup>3</sup>* ) and HDPE 0.93 to  
<sub>161</sub> 0.97 *g/cm<sup>3</sup>* ([Jonathan GUIDIGO1 et al., 2017](#)).

<sub>162</sub> **2.3 Printing process**

<sub>163</sub> **2.3.1 Establishing optimal parameters**

<sub>164</sub> Establishing optimum combinations of parameters is essential for better quality and me-  
<sub>165</sub> chanical properties of the printed parts ([Jaisingh Sheoran and Kumar, 2020](#)). According  
<sub>166</sub> to Oberloier et al. ([2022a](#)), particle swarm optimization (PSO) is an effective and time-  
<sub>167</sub> effective method for this purpose. The optimization of the 3-D printing parameters for the  
<sub>168</sub> rPET90//rHDPE10 material in the GigabotX was performed using the open-source PSO Ex-  
<sub>169</sub> perimenter platform (available in Linux), following the methodology developed by Oberloier  
<sub>170</sub> et al. ([2022a](#)). Three process benchmark artifacts were printed; line, plane, and cube. They  
<sub>171</sub> were modeled in CAD software Onshape CAD v1.150 and sliced using Prusaslicer v2.52.0.  
<sub>172</sub> Figure 3 presents the geometry models and dimensions.

Geometry	Lenght (mm)	width (mm)	height (mm)
Line	200	2	1
Plane	100	100	1
Cube	40	40	40

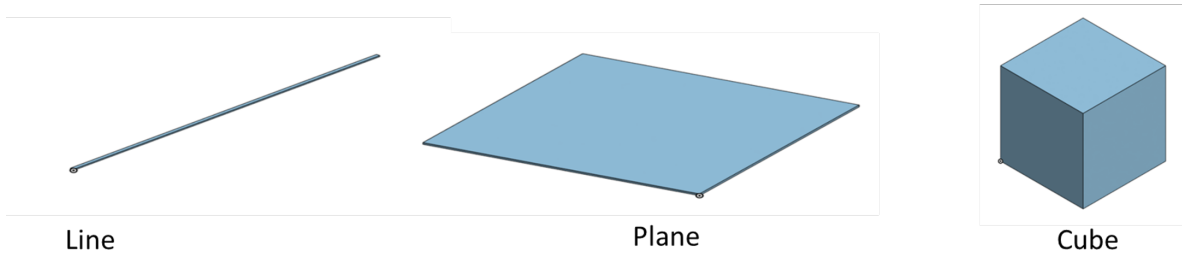


Figure 3: Dimensions and CAD models of the geometries used for parameters optimization.

<sub>173</sub> Four parameters were assessed: 1) the nozzle temperature, 2) bed temperature, 3) the printing  
<sub>174</sub> speed and 4) extrusion multiplier ([Oberloier et al., 2022b](#)). The initial parameters for the line  
<sub>175</sub> are presented in Table 1a while other parameters were obtained in preliminary experimental  
<sub>176</sub> work shown in Table 1.b. Finally, the PSO tuning parameters were found in the previous  
<sub>177</sub> PSO work ([Oberloier et al., 2022a](#)) Table 1.c.

Table 1: table 1

(a) Line optimization initial parameters

Variable	Min	Max	Guess	True/False	Description
T1	255	270	260	TRUE	Temperature Zone 1 on GigabotX
Tb	80	90	85	TRUE	Bed temperature
Ps	10	25	15	TRUE	Printing Speed
E	0.5	2	1	FALSE	Extrusion Multiplier

(b) Fixed parameters to perform printing parameters optimization based on PSO

Parameters	Value	Units
Layer height	0.5	mm
Width	2	mm
T2	230	°C
T3	220	°C
Cooling	0	%
Infill density	2	%

(c) Recommended parameters for PSO tuning

Variable	Value	Description
Kv	0.5	The emphasis given to the velocity component
Kp	1.0	The emphasis given to a particle's personal best position
Kg	2.0	The emphasis given to the swarm's group best position

### 178 2.3.2 Fused Granular Fabrication –FGF-

179 To print the raw material obtained, a 3-heat-zone modified open-source printer (Gigabot XL  
 180 re:3D, Houston, TX, USA) was used as illustrated in Figure 4. The machine is a single screw  
 181 extrusion-based 3-D printer capable of direct printing pellets, flakes or granules, with a nozzle  
 182 size of 1.75 mm. For this study, a chair was printed to evaluate the ability for the material  
 183 to 3-D print and the machine capacity to print large-objects such as a piece of furniture. The  
 184 ideal parameters found for the cube geometry were used to print the final part.

## 185 3 Results and discussion

### 186 3.1 Material characterization

187 Both polymeric components of the bottle as well as the blend were characterized and analyzed  
 188 to determine their properties using different methods as explained in the previous section.

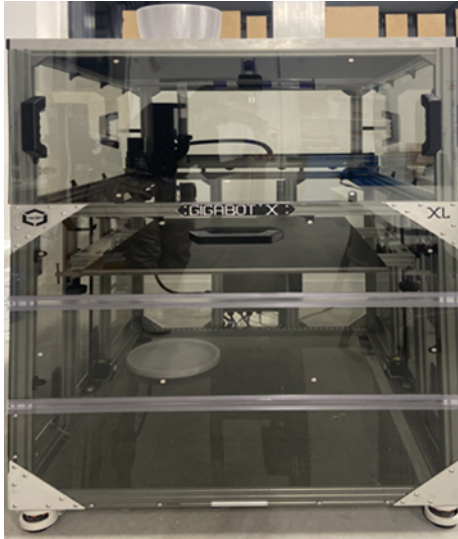


Figure 4: Fused granular fabrication printer Gigabot

<sup>189</sup> **3.1.1 Material particle size analysis (granulometry)**

<sup>190</sup> Previous studies demonstrated that particles with areas smaller than  $22 \text{ mm}^2$  were optimal  
<sup>191</sup> for print without jamming or under-extrusion problems (Woern et al., 2018). From the  
<sup>192</sup> experiments conducted, however, particles with areas above  $10 \text{ mm}^2$  clogged in the feeding  
<sup>193</sup> system and auger screw of the machine. Therefore, granulometry analysis was performed  
<sup>194</sup> using three different mesh sizes.

<sup>195</sup> Figure 5 shows the results obtained, where particles sifted at  $5 \text{ mm}$  had an average area  
<sup>196</sup> similar to the reference. There are, however, particles with areas over  $9 \text{ mm}^2$  which blocked  
<sup>197</sup> in the feeding and extrusion section. Particles sifted to  $1.5 \text{ mm}$  showed a distribution with  
<sup>198</sup> areas from 0 to proximately  $3 \text{ mm}^2$ , this area was considered too low for printing. Small  
<sup>199</sup> particles can completely melt in the first heat zone obstructing the consistent flow of other  
<sup>200</sup> particles and not allowing the pressure needed to extrude the melted particles lower in the  
<sup>201</sup> screw. Although flakes of  $3 \text{ mm}$  show a more dispersed distribution and slightly lower area  
<sup>202</sup> compared with the reference, those particles were found to be optimal for printing.

<sup>203</sup> The final objects, however, still displayed under-extrusion issues. For this reason, a crammer  
<sup>204</sup> was implemented (Little et al., 2020) as presented in Figure 6; which physically pushes

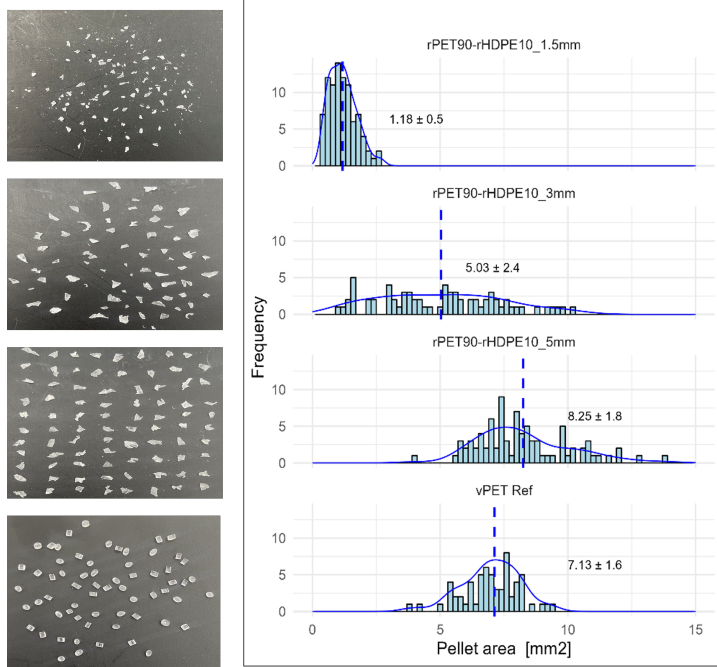


Figure 5: Granulometry analysis

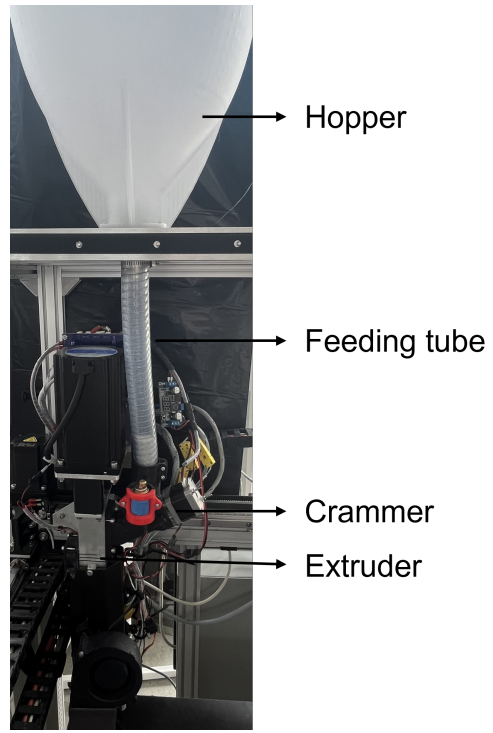


Figure 6: Gigabot feeding system

205 particles to the auger to convey them from feeding tube into the extruder. After the crammer  
 206 implementation under-extrusion issues were significantly decreased. It was concluded that  
 207 flakes with areas between  $1.5 \text{ mm}^2$  to  $10 \text{ mm}^2$  were optimum for print using a crammer able  
 208 to aid the feeding system.

### 209 3.1.2 Chemical analysis from FTIR

210 Chemical structure information of the materials was obtained using FTIR spectroscopy, which  
 211 provided analysis of the characteristic spectral bands of the polymers.

212 First, for the rPET (bottle) four characteristic bands can be observed Figure 7, one in  
 213  $1713\text{cm}^{-1}$  representing the  $C = O$  double bond, the  $C - O$  single bond ester at  $1240\text{cm}^{-1}$ ,  
 214  $1093\text{cm}^{-1}$  band corresponding to the methylene group and vibrations of the ester bond and  
 215 finally, a band  $722\text{cm}^{-1}$  the CH<sub>2</sub> rocking bending vibration.

216 Similar results were obtained in the literature for PET coming from recycled water bottles,

217 soda bottles and food containers (Zander et al., 2018). For rHDPE (caps), four charac-  
 218 teristic peaks were observed, the bond of C-H functional group in peaks  $2915\text{cm}^{-1}$  and  
 219  $2847\text{ cm}^{-1}$ , main bending mode of the -CH<sub>2</sub> in  $1465\text{ cm}^{-1}$  and CH<sub>2</sub> rocking bending vi-  
 220 bration at  $729\text{ cm}^{-1}$ . These results confirmed the chemical structures of starting materials.  
 221 Additionally, other indicative resonances besides those associated with the polymer structures  
 222 were not observed, concluding that additives or plasticizers in significative quantities were  
 223 not present in either sample. The spectrum of the printed blend (rPET90//rHDPE10) had  
 224 the same characteristic peaks as the bottle, confirming the PET dominant content. There  
 225 are, however, observable differences between  $1000\text{ cm}^{-1}$  and  $720\text{ cm}^{-1}$  and in the bond of C-  
 226 H ( $2915\text{ cm}^{-1}$  and  $2847\text{ cm}^{-1}$  peaks), confirming the presence of HDPE (cap). The shifting  
 227 observed can be attributed to interactions between both materials.

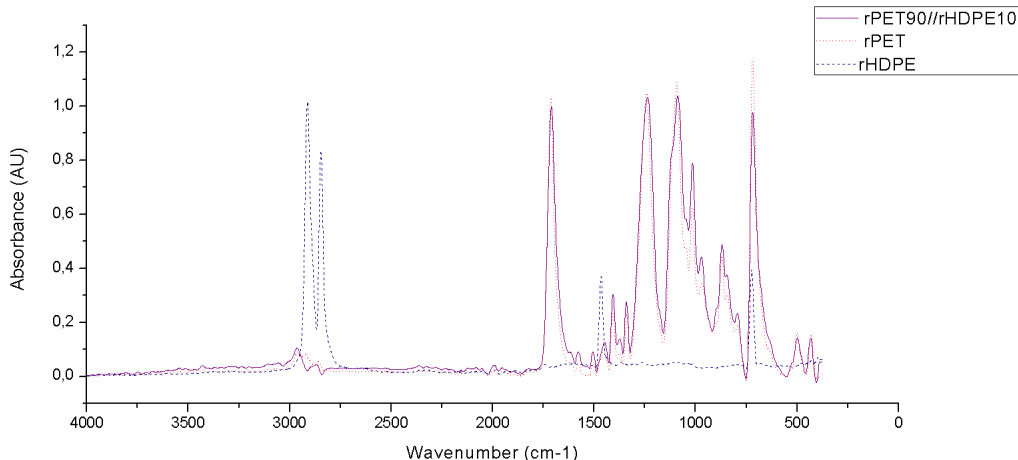


Figure 7: FTIR spectra of rPET, rHDPE and their blend

### 228 3.1.3 Thermal analysis DSC

229 The thermal properties of both recycled materials and their blend were characterized via  
 230 DSC to have a starting point for the 3-D printing process parameter optimization.  
 231 From the representative heating and cooling thermograms shown in Figure 8, two distinct  
 232 endothermic peaks are observed in the printed blend sample that are associated with fusion

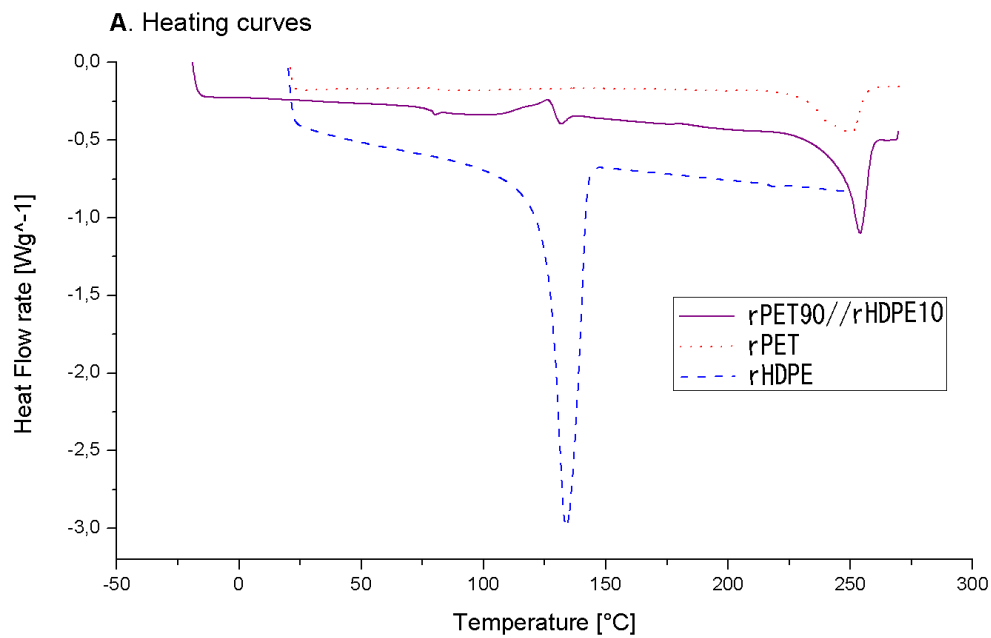
Table 2: Thermal analysis of rPET, rHDPE and their blend

Sample	Glass transition		Melting		Crystallization		% Crystallinity	
	Tg (°C)		Tm (°C)	ΔHm (J/g)	Tc (°C)	ΔHc (J/g)	ΔHcc (J/g)	Xc
rPET	82		249.9	31.6	196.7	34.8	-	22.6
rHDPE	-		133.8	172	118.7	158.5	-	58.7
rPET90//rHDPE10	77 / -		254/131.7	40.3/1.30	210.6/117.4	37.9/6.7	6.8	24.8 / 18.4

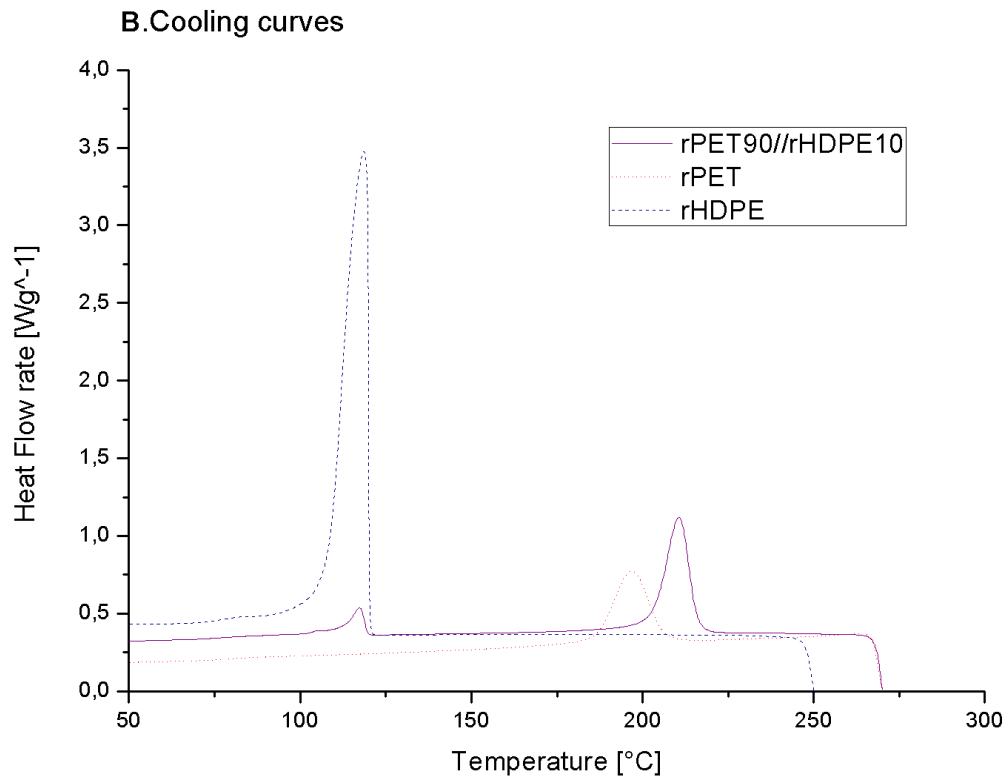
233 of the crystalline fractions of rHDPE and rPET, which confirms the immiscibility of both  
 234 materials. Moreover, a significant reduction in the enthalpy of fusion and crystallization of  
 235 the rHDPE in the blend is attributed to the low percentage of HDPE in the blend. The  
 236 observation of cold crystallization peak in the blend but not in the individual polymers,  
 237 however, can be attributed to an interaction between both polymers, where the rHDPE  
 238 might act as a nucleating agent. Table 2. list the thermal properties for rPET, rHDPE and  
 239 rPET90//rHDPE10. The melting point for rHDPE and rPET are 131.7 °C and 249.9 °C,  
 240 respectively and are similar to those found in the literature ([Chen et al., 2015](#); [Lei et al., 2009](#);  
 241 [Vaucher et al., 2022](#)). It is observed that the melting and crystallization temperature of rPET  
 242 shifted to a higher value, while slightly decreasing for rHDPE. In addition, the crystallization  
 243 of rPET was found be somewhat affected by the addition of rHDPE as it was increased 4%.  
 244 It is likely that the addition of the rHDPE acted as germination point for crystallization  
 245 ([Vaucher et al., 2022](#)). The slight changes in the rPET temperatures of fusion-crystallization  
 246 and degree of crystallinity showed the interaction of both polymers.

### 247 3.1.4 Rheology MFI

248 The melt flow index of the flakes was determined, enabling a fast and practical screening of the  
 249 viscosity of the material. Following the DSC results, the initial temperature to start the MFI  
 250 test was 250°C, however the material did not flow reliably so the temperature was increased by  
 251 5°C to enable the melt flow index of the rPET90//rHDPE10 to be determined. A temperature  
 252 of 260°C was also tested, however, the material flowed rapidly and the measurement could  
 253 not be reliably obtained. MFI tests were performed three times and the results of the  
 254 rPET90//rHDPE10 was a medium MFI  $39.4 \pm 2.4$  g/10min, which is roughly consistent



(a) Heating curves



(b) Cooling curve

Figure 8: DSC thermograms of recycled materials and blends

255 with values found in literature for rPET (Bustos Seibert et al., 2022; Langer et al., 2020;  
256 Nofar and Oğuz, 2019). This result suggests that the low percentage addition of HDPE do  
257 not highly impact the MFI value of rPET. As the material flowed at temperature of 255°C  
258 in the MFI, it provided the input temperature for 3-D printer parameters optimization.

259 **3.1.5 Density**

260 The density allows the estimation of cost, material use, time consumed and weight of the  
261 printing object in the slicer. This information is useful to find the accurate printing param-  
262 eters with the PSO experimenter as fitness is calculated as a function of the dimensional  
263 accuracy and weight of the printed object. Hence, density was useful to determine the weight  
264 of the geometries.

265 From calculations made after weight and measuring the rPET90//rHDPE10 injected object,  
266 the density of the material was found to be  $1.13 \text{ g/cm}^3$ . The inclusion of HDPE in the  
267 matrix polymer led to a slight decrease in its density, which is a common outcome when a  
268 polymer is mixed with a lower density polymer. However, if we consider a PET/HDPE blend  
269 with a mass ratio of 90/10, the calculated theoretical density is  $1.32 \text{ g/cm}^3$ . The observed  
270 decrease of 14% in the results could be attributed to factors such as experimental conditions  
271 and manual measurements.

272 **3.2 Particle swarm optimization (PSO) Experimenter**

273 Geometries were 3-D printed changing the parameters as expressed in the PSO Experimenter  
274 software. The fitness function is defined by the weighted sum of the dimensional measure-  
275 ments (length, width, height, and weight) of the printed object, where fitness below 0.1 was  
276 set as a desirable threshold. In the software five particles were established for one iteration,  
277 thus in one iteration five different parameters combinations were printed. The first geometry  
278 (line) was able to reach a fitness of  $< 0.1$  after six iterations for a total of thirty lines printed.  
279 The ideal parameters for this geometry are listed in column two of Table 3 and images of the  
280 resulting geometries are illustrated in Figure 9 .

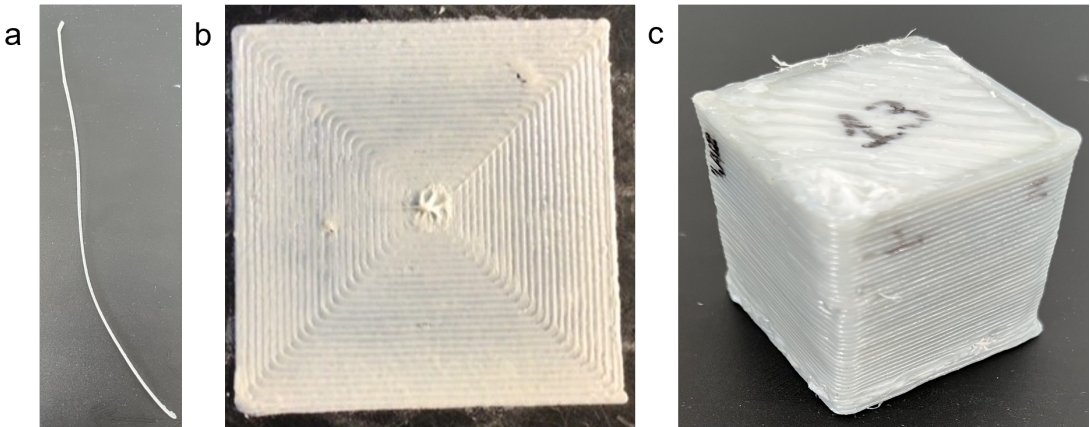


Figure 9: Images of the resulting geometries a) line, b) plane, c) cube

281 Afterwards, these parameters were used as initial guess for plane geometry, which reached  
 282 the desired fitness in the first iteration. Likewise, cubes were printed using the plane ideal  
 283 parameter as initial guess and optimal parameters, where found in the first iteration. Results  
 284 showed a significant change in the printing speed, which lowers at higher geometry complexity.  
 285 Moreover, the cube geometry required a higher extrusion multiplier to fill gaps and overcome  
 286 under-extrusion problems. The optimization of the parameters for the three geometries took  
 287 around 10h reducing the experimental time, compared with conventional methods. According  
 288 to Oberloier et al. (2022a) this time of experimentation can be reduced 97%. Indeed, the  
 289 efficacy of PSO in finding global optimum parameters is high, particularly when there is a  
 290 large or complex design space (Saad et al., 2019; Selvam et al., 2020).

291 Additionally, PSO converge to optimum solutions with fewer iterations than DoE methods  
 292 (Zhang et al., 2015) while mixing PSO with other meta-heuristic methods has shown higher  
 293 ability of predict and optimize parameters (e.g. minimize surface roughness(Shirmohammadi  
 294 et al., 2021), compressive strength and porosity of scaffolds (Asadi-Eydivand et al., 2016),  
 295 mechanical properties(Raju et al., 2019)). However, the DoE methods are still widely used  
 296 as they provide insight into the effects of individual design parameters and their interactions  
 297 while the ability to find interaction between the variables is not possible using PSO. In the  
 298 beginning of a set of optimization experiments, the complete understanding of the process  
 299 technique as well as the function settings might be complex. The methodology used in this

300 study, however, was easy to implement and the software has the advantage of being free, open  
301 source and user-friendly, lessening the initial difficulty. Thus, PSO demonstrated to be an  
302 effective and high accuracy prediction technique able to find the initial optimum parameters  
303 for rPET90//rHDPE10 material for FGF/FPF.

304 From the results it is observe that the optimal parameters may change depending of the object  
305 printed and each parameter has its own variation. One hypothesis is that geometry might  
306 play a role in parameter assignment and probably could be more visible in larger prints, yet  
307 this hypothesis needs further investigation. There are several physical mechanisms at play  
308 that would be expected to change optimal printing parameters based on the geometry and size  
309 of the object. For example, the cooling time and temperature history of a voxel will depend  
310 on the geometry of the printed object ([Cleeman et al., 2022](#)). Thus, to maintain the same  
311 thermal history the printing parameters must change as the geometry changes. This same  
312 effect of thermal history can also have more subtle impacts such as degree of crystallization  
313 even for PLA ([Wijnen et al., 2018](#)).

314 In addition, some physical effects of materials extrusion are magnified with scale. The most  
315 obvious is the impacts of thermal expansion and contraction. Small changes in contraction  
316 as a part cools may cause acceptable distortions for small prints, but these are magnified  
317 for large prints (e.g. causing deformation and in the worst cases delamination or loss of bed  
318 adhesion)([Shah et al., 2019](#)). Although, Roschli et al. ([2019](#)) showed the obstacles and  
319 possible solutions of the large-scale AM according to the way of the parts are designed the  
320 incidence of the geometry in the printing parameters needs far more detailed future studies.  
321 Specifically better models for mapping 3-D printing parameter optimizations of small printed  
322 objects to large volume objects is needed.

### 323 3.3 Functional object print

324 The ideal parameters found for the cube geometry were used as final parameters for print the  
325 case study product, except the print speed for the optimized line speed was used to decrease  
326 the printing time and delamination. This change was performed as according to the PSO

Table 3: Ideal printing parameters for fused granule fabrication of waste PET and HDPE blend made from shredded whole plastic water bottles

Variable	Line value	Planes value	Cube value	$\Delta$	Units
T1	258	263	264	6 $\pm$ 3.2	°C
Tb	86	82	84	4 $\pm$ 2	°C
Ps	21	14	10	11 $\pm$ 5.6	mm/s
E	1.07	0.87	1.32	0.5 $\pm$ 0.3	-

327 results the material is printable in a range of 10 to 20 mm/s. Additionally, the faster the  
 328 printing the lesser the time of cooling between the layers thus avoiding possible delamination  
 329 (Roschli et al., 2019), which is exacerbated for larger objects.

330 The Gigabot X successfully produced a piece of furniture from multi-material recycled water  
 331 bottles that included mixing HDPE and PET as shown in Figure 10 a.

332 The printing quality is acceptable as a prototype, proven the machine capacity of printing  
 333 large-scale functional objects where the chair was able to hold a child with a mass of 20 kg  
 334 comfortably as shown in Figure 10 f. The material, in the other hand, needs further evaluation  
 335 as the printed object showed weak bond strength between the adjacent layers (delamination  
 336 Figure 10 b). This is probably due to the difference in chemical properties of both materials or  
 337 immiscibility (Chu et al., 2022; William et al., 2021), high crystallinity (Verma et al., 2023)  
 338 and the large volume of the object as delamination issues were more visible at the time of  
 339 print the chair that in the parameters optimization process. Indeed, delamination presented  
 340 in the printing of a larger object can be attributed to the rapid cooling of the layers before  
 341 the material is once again deposited contrary of the cube printing where the small surface  
 342 allowing the adhesion of layers before there are completely cooled. This can even be an issue  
 343 for more popular 3-D printing materials like PLA from the print surface (Wijnen et al., 2018).  
 344 The addition of agents that reduce the interphase tension between polymers might help to  
 345 solve the delamination present and enhance the properties of the material (Dai et al., 1997;  
 346 Inoya et al., 2012; Kramer et al., 1994) as interfacial bond can be enhanced by polymer  
 347 modification (Gao et al., 2021) and viscosity decrement (Ko et al., 2019). Additionally,  
 348 while printing warping problems were observed, (Figure 10 c) which are likely caused by the

349 high crystallization rates of HDPE ([Schirmeister et al., 2019](#)). The use of Magigoo adhesive  
 350 (Thought3D Ltd., Paola, Malta) and the addition of a brim was tested in order to enable  
 351 bed adhesion, yet this solutions did not completely solve the problem. A previous study  
 352 showed that the use of a building plate made of thermoplastic elastomer SEBS allowed the  
 353 adhesion of the plastic and enables facile detachments of the printing object without breaking  
 354 or damaging ([Schirmeister et al., 2019](#)), suggesting a solution that needs further evaluation  
 355 in future work. Another visible issue present in the close angles of the printed object was  
 356 the shrinkage (Figure 10 d) which occurs during solidification and especially upon polymer  
 357 crystallization. Moreover, as is well-known, PET has hygroscopic tendencies and easily absorbs  
 358 atmosphere moisture making it difficult to extrude ([Bustos Seibert et al., 2022](#)) thus is likely  
 359 to break down in the presence of water, lowering the quality of the print. Before the chair  
 360 printing some samples showed brittle behavior and voids formation therefore, the material  
 361 was constantly dried and the hopper was closed in order to avoid moisture coming from  
 362 the environment helping to have a more printable material. Visually it can be observed  
 363 some vibration and ringing problems (Figure 10 e) caused by the machine upgrading, both  
 364 acceleration and jerk (maximum value of the instantaneous speed change) needs finer tuning.

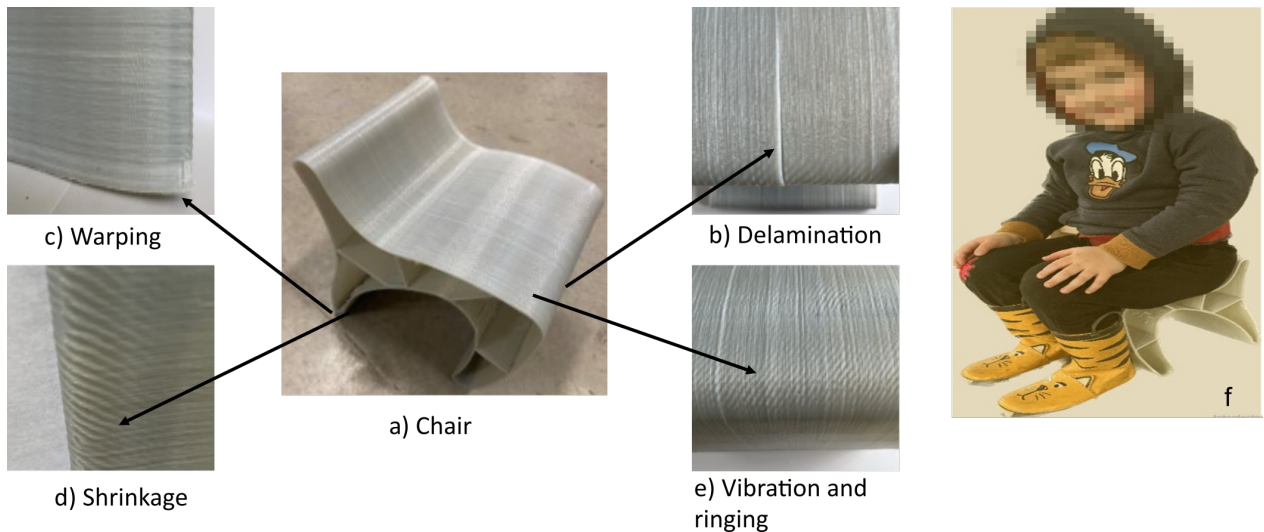


Figure 10: Finished children chair and printing issues

365 **3.3.1 Cost and environmental impact**

366 The printing time took 10 h and the printed object has a mass of 840 g. Due to the found  
367 optimized speed being low, the printing rate ( grams per hour) is low considering the machine  
368 that pellet printers have a typical throughput of 220 g to 9 kg per hour. The printing time  
369 could be improved by upgrading the extruder motor to a more powerful one. Besides, the  
370 energy required for 10 hr of 3-D printing was found to be 6 kW-hr resulting in a production  
371 cost of ~1.2 € in function of the electricity cost in France, without considering the material  
372 cost as bottles were obtained from post-consumers waste. When labor costs are not included  
373 the price was significative reduced (~88%) compared with those low cost found in the market.

374 The economics of fabricating the case study product remained competitive even if recycled  
375 plastic pellets or shreds are used, which can be found on the market from 1-10 €/kg. However,  
376 labor, maintenance and machine devaluation were not considered in the final price and are  
377 needed in future work for a complete economic evaluation.

378 Regarding the environmental impact, although this study does not evaluate the entire life  
379 cycle of the printed object, various scientific studies have already shown feasibility of dis-  
380 tributed recycling ([Kerdlap et al., 2022](#); [Santander et al., 2020](#)), the comparation between  
381 conventional and distributed manufacturing in terms of energy consumption and emissions  
382 ([Kreiger and Pearce, 2013](#)), environmental performance of AM ([Colorado et al., 2020](#); [Garcia  
383 et al., 2018](#)) and the appearance of DRAM as a source of raw material for diverse 3-D printers  
384 coming from post-consumer plastic waste in the form of either filament ([Hart et al., 2018](#);  
385 [Mikula et al., 2021](#); [Mohammed et al., 2017b](#); [Pakkanen et al., 2017b](#)) or granules ([Alexandre  
386 et al., 2020](#)).

387 Additionally, Caceres-Mendoza et al. ([2023](#)) has developed a complete life of cycle assess-  
388 ment of a DRAM system based on the production of PLA filament comparing virgin and  
389 recycled materials. Their environmental results showed a reduction of the impacts of produc-  
390 tion (climate change, fossil depletion, water depletion and potential eutrophication) of ~97%  
391 compared to virgin filament. These results, however, are dependent on the energy supply

<sup>392</sup> and can vary depending on location.

## <sup>393</sup> 4 Conclusion and future work

<sup>394</sup> This study analyzed the feasibility of using mixed post-consumer waste as feedstock material  
<sup>395</sup> for direct 3-D printing without compatibilization. The results showed the potential of mixing  
<sup>396</sup> solid waste plastics (PET/HDPE) for its use as feedstock material by printing a water bottle  
<sup>397</sup> with two incompatible polymers from the cap and body of the bottle. Additionally, the results  
<sup>398</sup> showed that a large-scale FGF 3-D printer was capable of producing a cost-effective functional  
<sup>399</sup> object from these mixed waste PET/HDPE plastics. Further research is needed in the analysis  
<sup>400</sup> of mechanical properties of the material as well as the possibilities of using compatibilizers  
<sup>401</sup> capable of enhancing the interphase tension between plastics and lower their crystallinity,  
<sup>402</sup> which might help improve performance and enhance material and 3-D printed part properties.  
<sup>403</sup> These factors increase in importance as the scale of the 3-D printed part increases. The  
<sup>404</sup> improvement of the material science of the approach can also offer an opportunity to improve  
<sup>405</sup> the quality of the printing printing time, lowering the energy consumption of the machine  
<sup>406</sup> and thus improving the economic viability of DRAM with mixed plastic waste.

<sup>407</sup> In addition, future work could assess the different types of combinations or blends between  
<sup>408</sup> commodity plastics using or not compatibilizer towards its printability, bringing out the  
<sup>409</sup> possibility of selection/sorting process elimination. In the same way, the development of  
<sup>410</sup> a methodology that allows the reproducibility of the process even in areas with limited  
<sup>411</sup> infrastructure opens up the potential of plastic revalorization using DRAM.

## <sup>412</sup> Declaration of competing

<sup>413</sup> The authors declare that they have no known competing financial interest or personal rela-  
<sup>414</sup> tionships that could have appeared to influence the work reported in this paper.

## **415 Acknowledgements**

416 This project has received funding from the European Union's Horizon 2020 research and  
417 innovation program under the grant agreement No 869952. The authors thank the LUE pro-  
418 gram for the financing of the thesis, the Lorraine Fab Living lab platform and the Thompson  
419 endowment.

420 **References**

- 421 Alexandre, A., Cruz Sanchez, F.A., Boudaoud, H., Camargo, M., Pearce, J.M., 2020. Me-  
422 chanical Properties of Direct Waste Printing of Polylactic Acid with Universal Pellets  
423 Extruder: Comparison to Fused Filament Fabrication on Open-Source Desktop Three-  
424 Dimensional Printers. *3D Printing and Additive Manufacturing* 7, 237–247. <https://doi.org/10.1089/3dp.2019.0195>
- 425
- 426 Anderson, I., 2017. Mechanical Properties of Specimens 3D Printed with Virgin and Recycled  
427 Polylactic Acid. *3D Printing and Additive Manufacturing* 4, 110–115. <https://doi.org/10.1089/3dp.2016.0054>
- 428
- 429 Asadi-Eydivand, M., Solati-Hashjin, M., Fathi, A., Padashi, M., Abu Osman, N.A., 2016.  
430 Optimal design of a 3D-printed scaffold using intelligent evolutionary algorithms. *Applied  
431 Soft Computing* 39, 36–47. <https://doi.org/10.1016/j.asoc.2015.11.011>
- 432 Attaran, M., 2020. 3D Printing Role in Filling the Critical Gap in the Medical Supply Chain  
433 during COVID-19 Pandemic. *American Journal of Industrial and Business Management*  
434 10, 988–1001. <https://doi.org/10.4236/ajibm.2020.105066>
- 435 Baechler, C., DeVuono, M., Pearce, J.M., 2013. Distributed recycling of waste polymer into  
436 RepRap feedstock. *Rapid Prototyping Journal* 19, 118–125. <https://doi.org/10.1108/13552541311302978>
- 437
- 438 Bowyer, A., 2014. 3D Printing and Humanity's First Imperfect Replicator. *3D Printing and  
439 Additive Manufacturing* 1, 4–5. <https://doi.org/10.1089/3dp.2013.0003>
- 440 Bustos Seibert, M., Mazzei Capote, G.A., Gruber, M., Volk, W., Osswald, T.A., 2022. Man-  
441 ufacturing of a PET Filament from Recycled Material for Material Extrusion (MEX).  
442 *Recycling* 7, 69. <https://doi.org/10.3390/recycling7050069>
- 443 Byard, D.J., Woern, A.L., Oakley, R.B., Fiedler, M.J., Snabes, S.L., Pearce, J.M., 2019.  
444 Green fab lab applications of large-area waste polymer-based additive manufacturing.  
445 *Additive Manufacturing* 27, 515–525. <https://doi.org/10.1016/j.addma.2019.03.006>
- 446 Caceres-Mendoza, C., Santander-Tapia, P., Cruz Sanchez, F.A., Troussier, N., Camargo,  
447 M., Boudaoud, H., 2023. Life cycle assessment of filament production in distributed  
448 plastic recycling via additive manufacturing. *Cleaner Waste Systems* 5, 100100. <https://doi.org/10.1016/j.clwas.2023.100100>
- 449
- 450 Carrete, I.A., Quiñonez, P.A., Bermudez, D., Roberson, D.A., 2021. Incorporating Textile-  
451 Derived Cellulose Fibers for the Strengthening of Recycled Polyethylene Terephthalate  
452 for 3D Printing Feedstock Materials. *Journal of polymers and the environment*.
- 453 Chen, R.S., Ab Ghani, M.H., Salleh, M.N., Ahmad, S., Tarawneh, M.A., 2015. Mechanical,  
454 water absorption, and morphology of recycled polymer blend rice husk flour biocomposites.  
455 *Journal of Applied Polymer Science* 132. <https://doi.org/10.1002/app.41494>
- 456 Chong, S., Pan, G.-T., Khalid, M., Yang, T.C.-K., Hung, S.-T., Huang, C.-M., 2017. Physi-  
457 cal Characterization and Pre-assessment of Recycled High-Density Polyethylene as 3D

- 458 Printing Material. *Journal of Polymers and the Environment* 25, 136–145. <https://doi.org/10.1007/s10924-016-0793-4>
- 459
- 460 Choong, Y.Y.C., Tan, H.W., Patel, D.C., Choong, W.T.N., Chen, C.-H., Low, H.Y., Tan, M.J., Patel, C.D., Chua, C.K., 2020. The global rise of 3D printing during the COVID-19 pandemic. *Nat Rev Mater* 5, 637–639. <https://doi.org/10.1038/s41578-020-00234-3>
- 461
- 462
- 463 Chu, J.S., Koay, S.C., Chan, M.Y., Choo, H.L., Ong, T.K., 2022. Recycled plastic filament made from post-consumer expanded polystyrene and polypropylene for fused filament fabrication. *Polymer Engineering & Science* 62, 3786–3795. <https://doi.org/10.1002/pen.26144>
- 464
- 465
- 466
- 467 Cleeman, J., Bogut, A., Mangrolia, B., Ripberger, A., Kate, K., Zou, Q., Malhotra, R., 2022. Scalable, Flexible and Resilient Parallelization of Fused Filament Fabrication: Breaking Endemic Tradeoffs in Material Extrusion Additive Manufacturing. *Additive Manufacturing* 102926. <https://doi.org/10.1016/J.ADDMA.2022.102926>
- 468
- 469
- 470
- 471 Colorado, H.A., Velásquez, E.I.G., Monteiro, S.N., 2020. Sustainability of additive manufacturing: The circular economy of materials and environmental perspectives. *Journal of Materials Research and Technology* 9, 8221–8234. <https://doi.org/10.1016/j.jmrt.2020.04.062>
- 472
- 473
- 474
- 475 Corsini, L., Aranda-Jan, C.B., Moultrie, J., 2022. The impact of 3D printing on the humanitarian supply chain. <https://doi.org/10.17863/CAM.51226>
- 476
- 477 Cruz Sanchez, F.A., Boudaoud, H., Camargo, M., Pearce, J.M., 2020. Plastic recycling in additive manufacturing: A systematic literature review and opportunities for the circular economy. *Journal of Cleaner Production* 264, 121602. <https://doi.org/10.1016/j.jclepro.2020.121602>
- 478
- 479
- 480
- 481 Cruz Sanchez, F.A., Boudaoud, H., Hoppe, S., Camargo, M., 2017. Polymer recycling in an open-source additive manufacturing context: Mechanical issues. *Additive Manufacturing* 17, 87–105. <https://doi.org/10.1016/j.addma.2017.05.013>
- 482
- 483
- 484 Dai, C.-A., Jandt, K.D., Iyengar, D.R., Slack, N.L., Dai, K.H., Davidson, W.B., Kramer, E.J., Hui, C.-Y., 1997. Strengthening Polymer Interfaces with Triblock Copolymers. *Macromolecules* 30, 549–560. <https://doi.org/10.1021/ma960396s>
- 485
- 486
- 487 Dertinger, S.C., Gallup, N., Tanikella, N.G., Grasso, M., Vahid, S., Foot, P.J.S., Pearce, J.M., 2020. Technical pathways for distributed recycling of polymer composites for distributed manufacturing: Windshield wiper blades. *Resources, Conservation and Recycling* 157, 104810. <https://doi.org/10.1016/j.resconrec.2020.104810>
- 488
- 489
- 490
- 491 Despeisse, M., Baumers, M., Brown, P., Charnley, F., Ford, S.J., Garmulewicz, A., Knowles, S., Minshall, T.H.W., Mortara, L., Reed-Tsochas, F.P., Rowley, J., 2017. Unlocking value for a circular economy through 3D printing: A research agenda. *Technological Forecasting and Social Change* 115, 75–84. <https://doi.org/10.1016/j.techfore.2016.09.021>
- 492
- 493
- 494
- 495 Evode, N., Qamar, S.A., Bilal, M., Barceló, D., Iqbal, H.M.N., 2021. Plastic waste and its management strategies for environmental sustainability. *Case Studies in Chemical and*
- 496

- 497 Environmental Engineering 4, 100142. <https://doi.org/10.1016/j.cscee.2021.100142>
- 498 Fontana, L., Giubilini, A., Arrigo, R., Malucelli, G., Minetola, P., 2022. Characterization  
499 of 3D Printed Polylactic Acid by Fused Granular Fabrication through Printing Accuracy,  
500 Porosity, Thermal and Mechanical Analyses. Polymers 14, 3530. <https://doi.org/10.3390/polym14173530>
- 501
- 502 Ford, S., Despesse, M., 2016. Additive manufacturing and sustainability: An exploratory  
503 study of the advantages and challenges. Journal of Cleaner Production 137, 1573–1587.  
504 <https://doi.org/10.1016/j.jclepro.2016.04.150>
- 505 Gaikwad, V., Ghose, A., Cholake, S., Rawal, A., Iwato, M., Sahajwalla, V., 2018. Transforma-  
506 tion of E-Waste Plastics into Sustainable Filaments for 3D Printing. ACS Sustainable  
507 Chemistry & Engineering 6, 14432–14440. <https://doi.org/10.1021/acssuschemeng.8b03105>
- 508
- 509 Gallup, N., Bow, J.K., Pearce, J.M., 2018. Economic Potential for Distributed Manufacturing  
510 of Adaptive Aids for Arthritis Patients in the U.S. Geriatrics 3, 89. <https://doi.org/10.3390/geriatrics3040089>
- 511
- 512 Gao, X., Qi, S., Kuang, X., Su, Y., Li, J., Wang, D., 2021. Fused filament fabrication  
513 of polymer materials: A review of interlayer bond. Additive Manufacturing 37, 101658.  
514 <https://doi.org/10.1016/j.addma.2020.101658>
- 515 Garcia, F.L., Moris, V.A. da S., Nunes, A.O., Silva, D.A.L., 2018. Environmental perfor-  
516 mance of additive manufacturing process – an overview. Rapid Prototyping Journal 24,  
517 1166–1177. <https://doi.org/10.1108/RPJ-05-2017-0108>
- 518 Geyer, R., 2020. Chapter 2 - Production, use, and fate of synthetic polymers, in: Letcher,  
519 T.M. (Ed.), Plastic Waste and Recycling. Academic Press, pp. 13–32. <https://doi.org/10.1016/B978-0-12-817880-5.00002-5>
- 520
- 521 Geyer, R., Jambeck, J.R., Law, K.L., 2017. Production, use, and fate of all plastics ever  
522 made. Science Advances 3, e1700782. <https://doi.org/10.1126/sciadv.1700782>
- 523 Grassi, G., Spagnolo, S.L., Paoletti, I., 2019. Fabrication and durability testing of a 3D  
524 printed façade for desert climates. Additive Manufacturing 28, 439.
- 525 Gwamuri, J., Franco, D., Khan, K.Y., Gauchia, L., Pearce, J.M., 2016. High-Efficiency Solar-  
526 Powered 3-D Printers for Sustainable Development. Machines 4, 3. <https://doi.org/10.3390/machines4010003>
- 527
- 528 Hart, K.R., Frketic, J.B., Brown, J.R., 2018. Recycling meal-ready-to-eat (MRE) pouches  
529 into polymer filament for material extrusion additive manufacturing. Additive Manufac-  
530 turing 21, 536–543. <https://doi.org/10.1016/j.addma.2018.04.011>
- 531 ImageJ, 2023. Image processing and analysis in java [WWW Document]. URL <https://imagej.nih.gov/ij/download.html> (accessed 6.13.2023).
- 532
- 533 Inoya, H., Wei Leong, Y., Klinklai, W., Thumsorn, S., Makata, Y., Hamada, H., 2012. Compatibilization of recycled poly (ethylene terephthalate) and polypropylene blends:  
534 Effect of polypropylene molecular weight on homogeneity and compatibility. Journal of
- 535

- 536 applied polymer science 124, 3947–3955.
- 537 Jaisingh Sheoran, A., Kumar, H., 2020. Fused Deposition modeling process parameters optimiza-  
538 tion and effect on mechanical properties and part quality: Review and reflection on  
539 present research. Materials Today: Proceedings, International Conference on Mechanical  
540 and Energy Technologies 21, 1659–1672. <https://doi.org/10.1016/j.matpr.2019.11.296>
- 541 Jonathan GUIDIGO1, Stéphane MOLINA2, Edmond C. ADJOVI3, André MERLIN  
542 4, DONNOT André5, Merlin SIMO TAGNE6, 2017. Polyethylene Low and High  
543 Density-Polyethylene Terephthalate and Polypropylene Blend as Matrices for Wood  
544 Flour, in: International Journal of Science and Research (IJSR). pp. 1069–1074.  
545 <https://doi.org/10.21275/ART20164296>
- 546 Jones, R., Haufe, P., Sells, E., Iravani, P., Olliver, V., Palmer, C., Bowyer, A., 2011. RepRap  
547 – the replicating rapid prototyper. Robotica 29, 177–191. <https://doi.org/10.1017/S026>  
548 357471000069X
- 549 Kerdlap, P., Purnama, A.R., Low, J.S.C., Tan, D.Z.L., Barlow, C.Y., Ramakrishna, S.,  
550 2022. Comparing the environmental performance of distributed versus centralized plastic  
551 recycling systems: Applying hybrid simulation modeling to life cycle assessment. Journal  
552 of Industrial Ecology 26, 252–271. <https://doi.org/10.1111/jiec.13151>
- 553 King, D., Babasola, A., Rozario, J., Pearce, J., 2014. Mobile Open-Source Solar-Powered  
554 3-D Printers for Distributed Manufacturing in Off-Grid Communities. Challenges in  
555 Sustainability 2. <https://doi.org/10.12924/cis2014.02010018>
- 556 Ko, Y.S., Herrmann, D., Tolar, O., Elspass, W.J., Brändli, C., 2019. Improving the filament  
557 weld-strength of fused filament fabrication products through improved interdiffusion. Addi-  
558 tive Manufacturing 29, 100815. <https://doi.org/10.1016/j.addma.2019.100815>
- 559 Kramer, E.J., Norton, L.J., Dai, C.-A., Sha, Y., Hui, C.-Y., 1994. Strengthening polymer  
560 interfaces. Faraday Discussions 98, 31–46. <https://doi.org/10.1039/FD9949800031>
- 561 Kratofil, L., Hrnjak-Murgić, Z., Jelencć, J., Andrićć, B., Kovacé, T., Merzel, V., 2006. Study  
562 of the compatibilizer effect on blends prepared from waste poly (ethylene-terephthalate)  
563 and high density polyethylene. International Polymer Processing 21, 328–335.
- 564 Kreiger, M.A., Mulder, M.L., Glover, A.G., Pearce, J.M., 2014. Life cycle analysis of dis-  
565 tributed recycling of post-consumer high density polyethylene for 3-D printing filament.  
566 Journal of Cleaner Production 70, 90–96. <https://doi.org/10.1016/j.jclepro.2014.02.009>
- 567 Kreiger, M., Pearce, J.M., 2013. Environmental Impacts of Distributed Manufacturing from  
568 3-D Printing of Polymer Components and Products. MRS Proceedings 1492, 85–90.  
569 <https://doi.org/10.1557/opl.2013.319>
- 570 Langer, E., Bortel, K., Waskiewicz, S., Lenartowicz-Klik, M., 2020. Methods of PET Recy-  
571 cling, Plasticizers Derived from Post-Consumer PET. <https://doi.org/10.1016/b978-0->  
572 [323-46200-6.00005-2](https://doi.org/10.1016/b978-0-323-46200-6.00005-2)
- 573 Lei, Y., Wu, Q., Zhang, Q., 2009. Morphology and properties of microfibrillar composites  
574 based on recycled poly (ethylene terephthalate) and high density polyethylene. Compos-

- 575       ites Part A: Applied Science and Manufacturing 40, 904–912. <https://doi.org/10.1016/j.compositesa.2009.04.017>
- 576
- 577 Lipsky, S., Przyjemska, A., Velasquez, M., Gershenson, J., 2019. 3D Printing for Humanitarian Relief: The Printer Problem, in: 2019 IEEE Global Humanitarian Technology Conference (GHTC). pp. 1–7. <https://doi.org/10.1109/GHTC46095.2019.9033053>
- 578
- 579 Little, H.A., Tanikella, N.G., J. Reich, M., Fiedler, M.J., Snabes, S.L., Pearce, J.M., 2020. Towards Distributed Recycling with Additive Manufacturing of PET Flake Feedstocks. Materials 13, 4273. <https://doi.org/10.3390/ma13194273>
- 580
- 581 Löschke, S.K., Mai, J., Proust, G., Brambilla, A., 2019. Microtimber: The Development of a 3D Printed Composite Panel Made from Waste Wood and Recycled Plastics. Digital Wood Design 24, 827–848. [https://doi.org/10.1007/978-3-030-03676-8\\_33](https://doi.org/10.1007/978-3-030-03676-8_33)
- 582
- 583 MacArthur, E., 2017. Beyond plastic waste. Science 358, 843–843. <https://doi.org/10.1126/science.aa06749>
- 584
- 585 Mikula, K., Skrzypczak, D., Izquierdo, G., Warchał, J., Moustakas, K., Chojnacka, K., Witek-Krowiak, A., 2021. 3D printing filament as a second life of waste plastics—a review. Environmental Science and Pollution Research 28, 12321–12333. <https://doi.org/10.1007/s11356-020-10657-8>
- 586
- 587 Mohammed, M.I., Das, A., Gomez-Kervin, E., Wilson, D., Gibson, I., 2017a. EcoPrinting: Investigating the Use of 100% Recycled Acrylonitrile Butadiene Styrene (ABS) for Additive Manufacturing. University of Texas at Austin.
- 588
- 589 Mohammed, M.I., Mohan, M., Das, A., Johnson, M.D., Badwal, P.S., McLean, D., Gibson, I., 2017b. A low carbon footprint approach to the reconstitution of plastics into 3D-printer filament for enhanced waste reduction. KnE Engineering 234–241. <https://doi.org/10.18502/keg.v2i2.621>
- 590
- 591 Mohammed, M.I., Wilson, D., Gomez-Kervin, E., Rosson, L., Long, J., 2018. EcoPrinting: Investigation of Solar Powered Plastic Recycling and Additive Manufacturing for Enhanced Waste Management and Sustainable Manufacturing, in: 2018 IEEE Conference on Technologies for Sustainability (SusTech). IEEE, pp. 1–6. <https://doi.org/10.1109/SusTech.2018.8671370>
- 592
- 593 Nofar, M., Oğuz, H., 2019. Development of PBT/Recycled-PET Blends and the Influence of Using Chain Extender. Journal of Polymers and the Environment 27, 1404–1417. <https://doi.org/10.1007/s10924-019-01435-w>
- 594
- 595 Novak, J.I., Loy, J., 2020. A critical review of initial 3D printed products responding to COVID-19 health and supply chain challenges. Emerald Open Research 2, 24. <https://doi.org/10.35241/emeraldopenres.13697.1>
- 596
- 597 Oberloier, S., Whisman, N.G., Pearce, J.M., 2022a. Finding Ideal Parameters for Recycled Material Fused Particle Fabrication-Based 3D Printing Using an Open Source Software Implementation of Particle Swarm Optimization. 3D Printing and Additive Manufacturing. <https://doi.org/10.1089/3dp.2022.0012>
- 598
- 599
- 600
- 601
- 602
- 603
- 604
- 605
- 606
- 607
- 608
- 609
- 610
- 611
- 612
- 613

- 614 Oberloier, S., Whisman, N.G., Pearce, J.M., 2022b. Finding Ideal Parameters for Recycled  
615 Material Fused Particle Fabrication-Based 3D Printing Using an Open Source Software  
616 Implementation of Particle Swarm Optimization. *3D Printing and Additive Manufactur-*  
617 *ing*. <https://doi.org/10.1089/3dp.2022.0012>
- 618 Pakkanen, J., Manfredi, D., Minetola, P., Iuliano, L., 2017a. About the Use of Recycled or  
619 Biodegradable Filaments for Sustainability of 3D Printing, in: Campana, G., Howlett,  
620 R.J., Setchi, R., Cimatti, B. (Eds.), Springer International Publishing, Cham, pp. 776–  
621 785. [https://doi.org/10.1007/978-3-319-57078-5\\_73](https://doi.org/10.1007/978-3-319-57078-5_73)
- 622 Pakkanen, J., Manfredi, D., Minetola, P., Iuliano, L., 2017b. About the Use of Recycled or  
623 Biodegradable Filaments for Sustainability of 3D Printing, in: Campana, G., Howlett,  
624 R.J., Setchi, R., Cimatti, B. (Eds.), *Sustainable Design and Manufacturing 2017, Smart*  
625 *Innovation, Systems and Technologies*. Springer International Publishing, Cham, pp.  
626 776–785. [https://doi.org/10.1007/978-3-319-57078-5\\_73](https://doi.org/10.1007/978-3-319-57078-5_73)
- 627 Pan, Y., Wu, G., Ma, H., Zhou, S., Zhang, H., 2020. Improved compatibility of PET/HDPE  
628 blend by using GMA grafted thermoplastic elastomer. *Polymer-Plastics Technology and*  
629 *Materials* 59, 1887–1898.
- 630 Pearce, J., Qian, J.-Y., 2022. Economic Impact of DIY Home Manufacturing of Consumer  
631 Products with Low-cost 3D Printing from Free and Open Source Designs. *European*  
632 *Journal of Social Impact and Circular Economy* 3, 1–24. <https://doi.org/10.13135/2704-9906/6508>
- 634 Petersen, E., Kidd, R., Pearce, J., 2017. Impact of DIY Home Manufacturing with 3D  
635 Printing on the Toy and Game Market. *Technologies* 5, 45. <https://doi.org/10.3390/te-chnologies5030045>
- 637 Petsiuk, A., Lavu, B., Dick, R., Pearce, J.M., 2022. Waste Plastic Direct Extrusion Hang-  
638 printer. *Inventions* 7, 70. <https://doi.org/10.3390/inventions7030070>
- 639 Pringle, A.M., Rudnicki, M., Pearce, J.M., 2018. Wood Furniture Waste-Based Recycled 3-D  
640 Printing Filament. *Forest Products Journal* 68, 86–95. <https://doi.org/10.13073/FPJ-D-17-00042>
- 642 Raju, M., Gupta, M.K., Bhanot, N., Sharma, V.S., 2019. A hybrid PSO–BFO evolutionary  
643 algorithm for optimization of fused deposition modelling process parameters. *Journal of*  
644 *Intelligent Manufacturing* 30, 2743–2758. <https://doi.org/10.1007/s10845-018-1420-0>
- 645 Rattan, R.S., Nauta, N., Romani, A., Pearce, J.M., 2023. Hangprinter for large scale additive  
646 manufacturing using fused particle fabrication with recycled plastic and continuous  
647 feeding. *HardwareX* 13, e00401. <https://doi.org/10.1016/j.ohx.2023.e00401>
- 648 Reich, M.J., Woern, A.L., Tanikella, N.G., Pearce, J.M., 2019. Mechanical Properties and  
649 Applications of Recycled Polycarbonate Particle Material Extrusion-Based Additive Man-  
650 ufacturing. *Materials* 12, 1642. <https://doi.org/10.3390/ma12101642>
- 651 Rett, J.P., Traore, Y.L., Ho, E.A., 2021. Sustainable Materials for Fused Deposition Modeling  
652 3D Printing Applications. *Advanced Engineering Materials* 23, 2001472. <https://doi.or>

- 653 [g/10.1002/adem.202001472](https://doi.org/10.1002/adem.202001472)
- 654 Romani, A., Rognoli, V., Levi, M., 2021. Design, Materials, and Extrusion-Based Additive  
655 Manufacturing in Circular Economy Contexts: From Waste to New Products. Sustainability  
656 13, 7269. <https://doi.org/10.3390/su13137269>
- 657 Roschli, A., Gaul, K.T., Boulger, A.M., Post, B.K., Chesser, P.C., Love, L.J., Blue, F., Borish,  
658 M., 2019. Designing for Big Area Additive Manufacturing. Additive Manufacturing 25,  
659 275–285. <https://doi.org/10.1016/j.addma.2018.11.006>
- 660 Saad, M.S., Nor, A.M., Baharudin, M.E., Zakaria, M.Z., Aimani, A.F., 2019. Optimization of  
661 surface roughness in FDM 3D printer using response surface methodology, particle swarm  
662 optimization, and symbiotic organism search algorithms. The International Journal of  
663 Advanced Manufacturing Technology 105, 5121–5137. <https://doi.org/10.1007/s00170-019-04568-3>
- 664 Salmi, M., Akmal, J.S., Pei, E., Wolff, J., Jaribion, A., Khajavi, S.H., 2020. 3D Printing  
665 in COVID-19: Productivity Estimation of the Most Promising Open Source Solutions in  
666 Emergency Situations. Applied Sciences 10, 4004. <https://doi.org/10.3390/app10114004>
- 667 Santander, P., Cruz Sanchez, F.A., Boudaoud, H., Camargo, M., 2020. Closed loop supply  
668 chain network for local and distributed plastic recycling for 3D printing: A MILP-based  
669 optimization approach. Resources, Conservation and Recycling 154, 104531. <https://doi.org/10.1016/j.resconrec.2019.104531>
- 670 Savonen, B.L., Mahan, T.J., Curtis, M.W., Schreier, J.W., Gershenson, J.K., Pearce, J.M.,  
671 2018. Development of a Resilient 3-D Printer for Humanitarian Crisis Response. Technologies  
672 6, 30. <https://doi.org/10.3390/technologies6010030>
- 673 Schirmeister, C.G., Hees, T., Licht, E.H., Mülhaupt, R., 2019. 3D printing of high density  
674 polyethylene by fused filament fabrication. Additive Manufacturing 28, 152–159. <https://doi.org/10.1016/j.addma.2019.05.003>
- 675 Sells, E., Smith, Z., Bailard, S., Bowyer, A., Olliver, V., 2009. RepRap: The Replicating  
676 Rapid Prototyper - maximizing customizability by breeding the means of production,  
677 in: Piller, F.T., Tseng, M.M. (Eds.), Handbook of Research in Mass Customization and  
678 Personalization. World Scientific, pp. 568–580.
- 679 Selvam, A., Mayilswamy, S., Whenish, R., 2020. Strength Improvement of Additive Manufac-  
680 turing Components by Reinforcing Carbon Fiber and by Employing Bioinspired Interlock  
681 Sutures. Journal of Vinyl and Additive Technology 26, 511–523. <https://doi.org/10.1002/vnl.21766>
- 682 Shah, J., Snider, B., Clarke, T., Kozutsky, S., Lacki, M., Hosseini, A., 2019. Large-scale  
683 3D printers for additive manufacturing: Design considerations and challenges. The  
684 International Journal of Advanced Manufacturing Technology 104, 3679–3693. <https://doi.org/10.1007/s00170-019-04074-6>
- 685 Shirmohammadi, M., Goushchi, S.J., Keshtiban, P.M., 2021. Optimization of 3D printing  
686 process parameters to minimize surface roughness with hybrid artificial neural network

- 692 model and particle swarm algorithm. *Progress in Additive Manufacturing* 6, 199–215.  
693 <https://doi.org/10.1007/s40964-021-00166-6>
- 694 Siltaloppi, J., Jähi, M., 2021. Toward a sustainable plastics value chain: Core conundrums  
695 and emerging solution mechanisms for a systemic transition. *Journal of Cleaner Production*  
696 315, 128113. <https://doi.org/10.1016/j.jclepro.2021.128113>
- 697 Soares, J., Miguel, I., Venâncio, C., Lopes, I., Oliveira, M., 2021. Public views on plastic  
698 pollution: Knowledge, perceived impacts, and pro-environmental behaviours. *Journal of*  
699 *Hazardous Materials* 412, 125227. <https://doi.org/10.1016/j.jhazmat.2021.125227>
- 700 Taghavi, S.K., Shahrajabian, H., Hosseini, H.M., 2018. Detailed comparison of compatibi-  
701 lizers MAPE and SEBS-g-MA on the mechanical/thermal properties, and morphology  
702 in ternary blend of recycled PET/HDPE/MAPE and recycled PET/HDPE/SEBS-g-MA.  
703 *Journal of Elastomers & Plastics* 50, 13–35.
- 704 Van de Voorde, B., Katalagarianakis, A., Huysman, S., Toncheva, A., Raquez, J.-M., Duretek,  
705 I., Holzer, C., Cardon, L., Bernaerts, K., V, Van Hemelrijck, D., Pyl, L., Van Vlierberghe,  
706 S., 2022. Effect of extrusion and fused filament fabrication processing parameters of recy-  
707 cled poly(ethylene terephthalate) on the crystallinity and mechanical properties. *Additive*  
708 *Manufacturing* 50. <https://doi.org/10.1016/j.addma.2021.102518>
- 709 Vaucher, J., Demongeot, A., Michaud, V., Leterrier, Y., 2022. Recycling of Bottle Grade  
710 PET: Influence of HDPE Contamination on the Microstructure and Mechanical Perfor-  
711 mance of 3D Printed Parts. *Polymers* 14, 5507. <https://doi.org/10.3390/polym14245507>
- 712 Verma, N., Awasthi, P., Gupta, A., Banerjee, S.S., 2023. Fused Deposition Modeling of  
713 Polyolefins: Challenges and Opportunities. *Macromolecular Materials and Engineering*  
714 308, 2200421. <https://doi.org/10.1002/mame.202200421>
- 715 Wijnen, B., Sanders, P., Pearce, J.M., 2018. Improved model and experimental validation  
716 of deformation in fused filament fabrication of polylactic acid. *Progress in Additive*  
717 *Manufacturing* 3, 193–203. <https://doi.org/10.1007/s40964-018-0052-4>
- 718 William, L.J.W., Koay, S.C., Chan, M.Y., Pang, M.M., Ong, T.K., Tshai, K.Y., 2021.  
719 Recycling Polymer Blend made from Post-used Styrofoam and Polypropylene for Fuse  
720 Deposition Modelling. *Journal of Physics: Conference Series* 2120, 012020. <https://doi.org/10.1088/1742-6596/2120/1/012020>
- 722 Woern, A.L., McCaslin, J.R., Pringle, A.M., Pearce, J.M., 2018. RepRapable Recyclebot:  
723 Open source 3-D printable extruder for converting plastic to 3-D printing filament. *Hard-  
724 wareX* 4, e00026. <https://doi.org/10.1016/j.ohx.2018.e00026>
- 725 Wong, J.Y., 2015. Ultra-Portable Solar-Powered 3D Printers for Onsite Manufacturing of  
726 Medical Resources. *Aerospace Medicine and Human Performance* 86, 830–834. <https://doi.org/10.3357/AMHP.4308.2015>
- 728 Zander, N.E., Gillan, M., Burckhard, Z., Gardea, F., 2019. Recycled polypropylene blends  
729 as novel 3D printing materials. *Additive Manufacturing* 25, 122–130. <https://doi.org/10.1016/j.addma.2018.11.009>

- 731 Zander, N.E., Gillan, M., Lambeth, R.H., 2018. Recycled polyethylene terephthalate as a  
732 new FFF feedstock material. Additive Manufacturing 21, 174–182. <https://doi.org/10.1016/j.addma.2018.03.007>
- 733
- 734 Zhang, Y., Wang, S., Ji, G., 2015. A Comprehensive Survey on Particle Swarm Optimization  
735 Algorithm and Its Applications. Mathematical Problems in Engineering 2015, e931256.  
736 <https://doi.org/10.1155/2015/931256>
- 737 Zhong, S., Pearce, J.M., 2018. Tightening the loop on the circular economy: Coupled dis-  
738 tributed recycling and manufacturing with recyclebot and RepRap 3-D printing. Re-  
739 sources, Conservation and Recycling 128, 48–58. <https://doi.org/10.1016/j.resconrec.2017.09.023>
- 740